Large plasmonic field enhancement on hydrogen-absorbing transition metals at lower frequencies: Implications for hydrogen storage, sensing, and nuclear fusion

Cite as: J. Appl. Phys. **126**, 023102 (2019); https://doi.org/10.1063/1.5091723
Submitted: 05 February 2019 . Accepted: 18 June 2019 . Published Online: 08 July 2019

Norihiko Fukuoka, and Katsuaki Tanabe

Journal of Applied Physics ARTICLE scitation.org/journal/jap

Large plasmonic field enhancement on hydrogen-absorbing transition metals at lower frequencies: Implications for hydrogen storage, sensing, and nuclear fusion

Cite as: J. Appl. Phys. **126**, 023102 (2019); doi: 10.1063/1.5091723
Submitted: 5 February 2019 · Accepted: 18 June 2019 ·
Published Online: 8 July 2019

Norihiko Fukuoka and Katsuaki Tanabe[a)]

AFFILIATIONS

Department of Chemical Engineering, Kyoto University, Nishikyo, Kyoto 615-8510, Japan

[a)]**E-mail:** tanabe@cheme.kyoto-u.ac.jp

ABSTRACT

The plasmonic enhancement of electromagnetic field energy density around planar surfaces of hydrogen-absorbing transition metals, Pd, Ti, and Ni, has been quantitatively investigated, to explore the use of plasmonics in the forthcoming hydrogen economy. We have observed that a large degree of energy focusing, with the enhancement factor over several hundreds, is available for these transition metals in the microwave region, even surpassing the enhancement for noble metals. This finding could potentially lead to technological progress in various hydrogen-related energy applications including hydrogen storage, sensing, and nuclear fusion.

I. INTRODUCTION

A group of transition metals such as Pd, Ti, and Ni are promising for their high ability to absorb hydrogen, for applications including hydrogen energy storage[1–4] and sensing.[2,5] Free electrons in metals, particularly around metallic surfaces or interfaces with dielectric media, exhibit a strong interaction with electromagnetic fields or light in the form of collective oscillation, named "surface plasmons."[6–12] Surface-plasmon-induced electromagnetic field enhancement on metal surfaces can be utilized for the enhancement of hydrogen absorption rate[13] and optical detection sensitivity[14–16] for applications such as hydrogen storage.

Laser fusion technology can potentially provide an ideal energy source for humans.[17–21] One of the most crucial issues hindering its practical realization at present is the low energy-coupling efficiency between the heating laser and the fuel target. Energy focusing into the fuel targets, achieved by attaching metallic cone guiding materials in the vicinity of targets, has been implemented to some extent,[18,19] but further focusing, particularly inside the targets, is required. The possibility of realizing compact nuclear-fusion reactors using deuterium-absorbed metals has also been investigated.[22–27] The density of the triggering energy supplied to deuterium-metal systems to activate the nuclear-fusion reaction may be one of the key factors for producing a smooth and reproducible initiation of the reaction.

Noble metals such as Au, Ag, and Cu are known to exhibit large plasmonic field enhancements at optical frequencies and have been considerably investigated in the context of plasmonics, both experimentally and theoretically.[6–12,28] However, there is an inadequate study of the surface-plasmon behavior of transition metal surfaces, particularly for longer wavelengths, and thus, this behavior is not well understood. The microwave region is important for applications such as heating, sensing, imaging, communication, and healthcare, and, therefore, a number of low-frequency plasmonics studies have been carried out for noble metals.[29–31] Previously, we evaluated plasmonic field enhancement factors for transition metals in the optical frequency region, with the results indicating a decent degree of field enhancement, with the enhancement factor up to a couple of tens.[32] In the present study, we present electromagnetic calculations at lower frequencies, with significantly higher degrees of field enhancements, particularly for hydrogen-absorbing transition metals, Pd, Ti, and Ni.

II. THEORY AND CALCULATION METHODS

We calculated the field enhancement factors, which represent the intensity ratios for fields around the object to those in the absence of the object (metals in this case), or the original incident fields, for planar metals in air, H_2, or vacuum, and H_2O. These calculations, which are based on the classical electromagnetic field theory, quantitatively show how much energy can be concentrated from the incident optical or electric power. We adopted the scheme to derive the maximum field enhancement described in Ref. 33. Having removed the noble-metal approximation in Ref. 33 (as described in detail later), we fully calculated the field enhancement factors for Pd, Ti, and Ni. Figure 1 shows a schematic cross-sectional view of the system under consideration. Let ε_1 and ε_2 be the frequency-dependent complex permittivities or dielectric functions of the surrounding medium and the metal, respectively, and let θ be the incident angle. We assumed an incidence of a p-polarized plane wave as the original electromagnetic field and its coupling into a surface-plasmon mode to determine the maximum field enhancement factors. The method used to calculate the field enhancement factors is described in Ref. 32. We extend the calculation region to the infrared or microwave frequencies in the present study, in contrast to the optical frequency region studied in Ref. 32. In short, the field enhancement factor is calculated as

$$\eta \equiv \frac{|\vec{E}_{SP}(0^+)|^2}{|\vec{E}_0|^2} = \frac{c(|q_1|^2 + |k_{SP}|^2)\cos\theta(1-R)}{\omega\varepsilon_1^{1/2}k_{SP}''\mathrm{Re}\left\{\dfrac{k_{SP}(\varepsilon_1 q_1' + \varepsilon_2 q_2')}{\varepsilon_2 q_1' q_2'}\right\}}. \quad (1)$$

Here, $\vec{E}_{SP}$ is the electric field for the surface-plasmon mode; $\vec{E}_0$ is the electric field of the incident wave, or, namely, the external field; c is the speed of light; ω is the frequency of the field; R is the reflectivity at the metal surface; q_1 and q_2 are the complex wave vectors in the z direction in the surrounding medium and the metal, respectively; and k_{SP} represents the complex wave vector of the surface-plasmon mode in the x direction. The wave vectors were calculated by

$$q_j = \frac{\omega}{c}\left(\frac{-\varepsilon_j^2}{\varepsilon_1 + \varepsilon_2}\right)^{1/2} \quad (j = 1, 2), \quad (2)$$

$$k_{SP} = \frac{\omega}{c}\left(\frac{\varepsilon_1\varepsilon_2}{\varepsilon_1 + \varepsilon_2}\right)^{1/2}. \quad (3)$$

The real and imaginary parts of complex quantities are indicated by primes and double primes, respectively. Note that this field enhancement factor is defined as the ratio of field "intensities" and not field "magnitudes." Weber and Ford used an approximation, $\varepsilon_2'' \ll -\varepsilon_2'$, in the derivation of the field enhancement factor. They rationalized this approximation by the nonlossy nature of noble metals, which were the only materials they dealt with in Ref. 33, so they ended up with a much simpler formula. In contrast, we fully calculated the enhancement factors as given in Eq. (1), removing the approximation to properly deal with the relatively lossy metals in this study.

While the Drude model is widely used for dielectric functions of metals for plasmonic electromagnetic calculations,[34,35] we adopted polynomial fitting for the experimentally measured frequency-dependent optical constant data listed in Refs. 36 (for H_2O) and 37 (for metals) for the calculations in this article, as summarized in the Appendix. This is because it is difficult to fit the formalism of the Drude model to the dispersion of dielectric functions of realistic metallic materials for entire frequencies through the ultraviolet to the infrared, specifically for the higher energy region due to the bound-charge contribution.[38] Figures 2(a) and 2(b) show the polynomial fit used in this study for the real and imaginary parts, respectively, of the dielectric functions for the metals we dealt with in this study, Au, Ag, Cu, Pd, Ti, and Ni, and also H_2O [Figs. 2(c) and 2(d)]. We assumed that $\varepsilon' = 1$ and $\varepsilon'' = 0$ throughout the entire frequencies for air, H_2, and vacuum. For Au, Ag, and Cu at higher frequencies, we used the fitting functions in Ref. 10 for the computations in this paper.

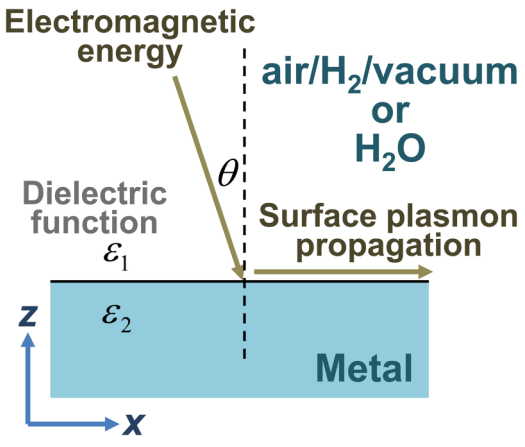

FIG. 1. Schematic spatial cross-sectional view of the material system considered in this study for the calculations of field enhancement factors.

III. RESULTS AND DISCUSSION

Figure 3 shows the calculated spectra of field enhancement factors at the metal surfaces for Au, Ag, Cu, Pd, Ti, and Ni in air, H_2, or vacuum [Fig. 3(a)] and H_2O [Fig. 3(b)]. We assumed normal incidence ($\theta = 0$) and perfect coupling of the external field to the surface-plasmon mode ($R = 0$) to determine the maximum possible enhancement in this calculation. The difference in the plotted wavelength ranges among the metals is simply due to the difference in the available data in Ref. 37. The monotonic increase in the field enhancement factors with the wavelength for Au, Ag, and Cu observed in Fig. 3(a) is consistent with the results in Ref. 33 for the range up to 700 nm, handled therein. In addition, for all the six metals presently studied, we did not observe any surface-plasmon resonance behavior in the dispersion relation of k_{SP} throughout the wavelengths for both cases in air and H_2O, except for the well-known resonance around 350 and 500 nm for Ag and Au, respectively. Local energy enhancement at the

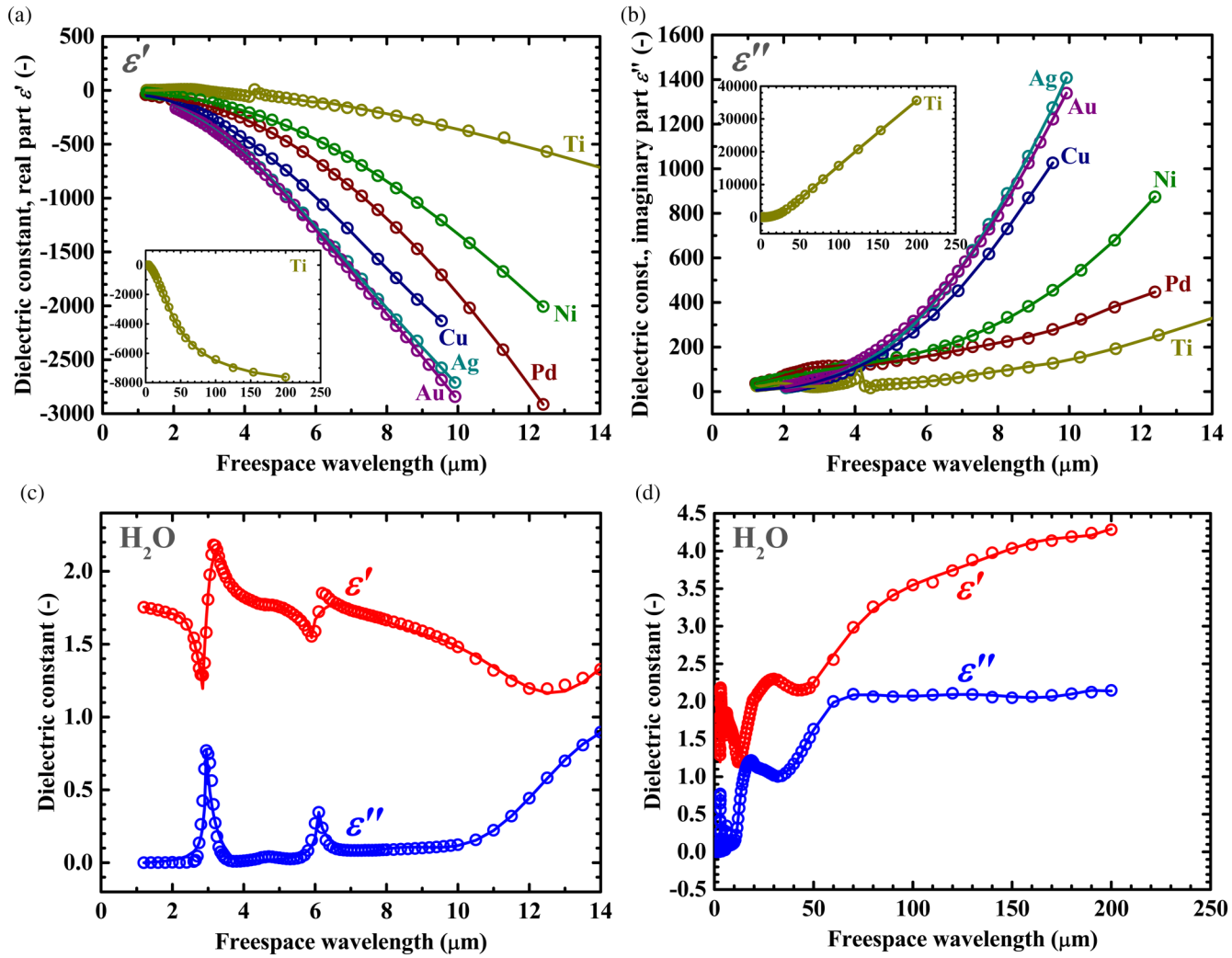

FIG. 2. (a) Real and (b) imaginary parts of the dielectric functions for Au, Ag, Cu, Pd, Ti, and Ni. (c) and (d) Dielectric functions for H_2O for varied wavelength regions. The dielectric constants are unitless. The insets of (a) and (b) are the plots for Ti for further wavelength regions. The dots are the empirical values from Refs. 36 and 37, and the lines are the polynomial fit used for the calculations in this study. The fitting equations are found in the Appendix.

metal/dielectric interfaces of a certain degree is seen in the spectra in Fig. 3. In this way, the metal surfaces can concentrate optical or electromagnetic energy in their vicinity. Among the metal elements we calculated, the noble metals Au, Ag, and Cu are known to exhibit distinctively higher field enhancement factors than other metals in the higher frequency region (i.e., shorter wavelengths) due to their high conductivity.[10,33,39] A certain level of field enhancement, however, is still attainable even for the hydrogen-absorbing transition metals Pd, Ti, and Ni, as seen in Fig. 3. Conversely, in the lower frequency or longer wavelength region for air, H_2, or vacuum, the field enhancements for Pd, Ti, and Ni are surprisingly significantly higher and even surpass those of noble metals, as seen in Fig. 3(a). This result can be attributed to significantly smaller ε'', causing lower propagation loss or longer lifetime of the surface-plasmon mode, of Pd, Ti, and Ni than those of Au, Ag, and Cu at lower frequencies, as seen in Fig. 2(b); n.b., the magnitude relation of ε'' is reversed around 3 μm. Remarkably, the field enhancement factor for Pd is over 700, even for the frequency region whose dielectric function data can be evaluated thus far. It should be noted that the field enhancement factors for Pd, Ti, and Ni still show increasing tendency even at the lower frequency edge in our calculation, while Au, Ag, and Cu reach the plateau. Therefore, the plasmonic electromagnetic field enhancement of Pd, Ti, and Ni may be expected to increase even further at far lower frequencies. In contrast, however, the field enhancement factors for H_2O are significantly smaller at lower frequencies for all the metals, as seen in

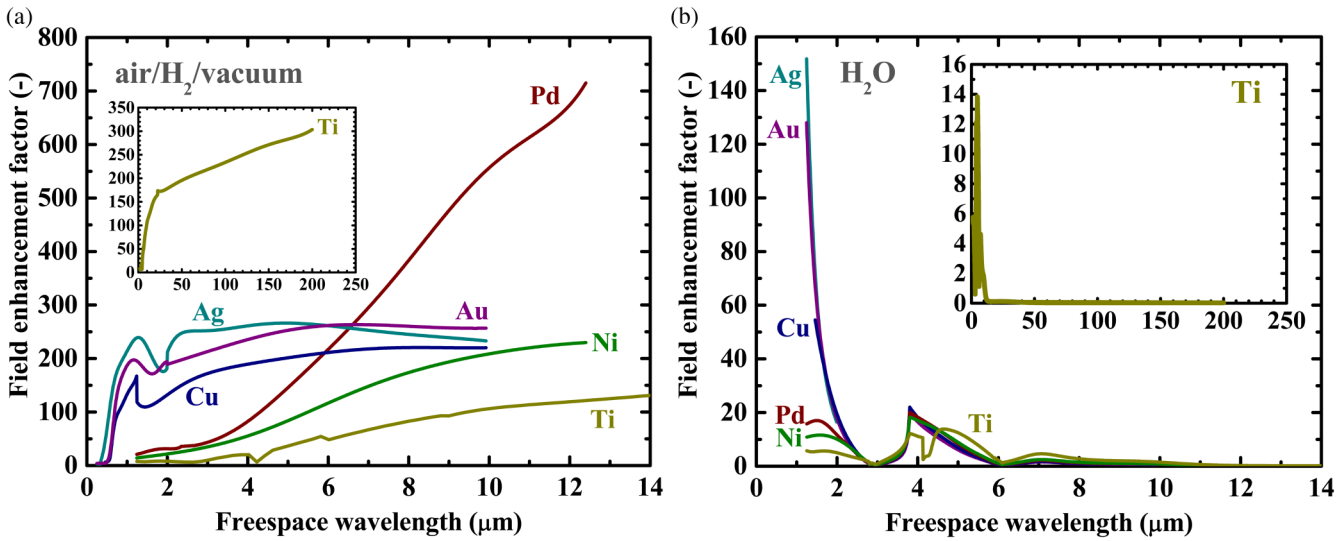

FIG. 3. Calculated electromagnetic field enhancement factors on Au, Ag, Cu, Pd, Ti, and Ni surfaces in (a) air/H_2/vacuum and (b) H_2O. The insets are the plots for Ti for further wavelength regions.

Fig. 3(b). This rather unexpected result can be attributed to the fact that the increase in ε_1'' of H_2O with wavelength, seen in Figs. 2(c) and 2(d), significantly enlarges k_{SP}'', i.e., fast decay of surface-plasmon polariton mode propagating at the metal/H_2O interface, especially due to the large absolute values of ε_2' and ε_2'' of the metals at lower frequencies, seen in Figs. 2(a) and 2(b).

It should be noted that the coupling of incident electromagnetic or optical energy into surface-plasmon modes does not occur at perfectly smooth metal surfaces. In this case, there is no enhancement of the electromagnetic energy, due to the extremely large reflectivity at the metal surface. Surface structures with scales smaller than the wavelength of the external or incident fields are required for efficient plasmon coupling to induce the enhancement effect.[40–42] The surface structure is not necessarily periodic, but random roughness can also generate surface plasmons.[40,43,44] For example, there may be some intrinsic micro/nanoscale roughness on regular metal surfaces. It is, therefore, expected that there is still some surface-plasmon electromagnetic enhancement effect even for normal metal materials, but not necessarily with particularly prepared surfaces intentionally micro/nano-engineered for plasmon coupling.

Note that the plasmonic energy-focusing scheme we studied in this paper is applicable not only to electric-field applications (through the application of electrical bias such as electrochemical batteries or electrolysis cells) but also to optical excitation sources such as lasers, since the electromagnetic field enhancement is equivalent for both systems. In this work, we calculated the field enhancement factors for a certain range of frequencies, but extrapolations to longer wavelengths provide estimates for cases such as the DC field or continuous-wave power application. This sort of optical or electromagnetic numerical model, incidentally, is simple and flexible for connecting to other models and may be employed to construct a comprehensive model by combining it with transport and reaction submodels,[45,46] for instance.

This paper aims to give a conceptual understanding of the nature of the concentration of electromagnetic fields around metallic substances. As a result, we assumed that the case of a single metal/dielectric interface geometry is suitable due to its relatively straightforward computation and analysis. Therefore, in the present work, we showed calculations only for such a single-surface system for the sake of simplicity as a preliminary investigation, but surface plasmons located in between multiple metal structures with nanoscale separation distances, or so-called "gap plasmons,"[47–49] would provide even higher field enhancement factors on conditions. This gap-plasmon effect will be discussed in future work.

The plasmonic field enhancement effect we calculated in this work can be potentially applied, for example, to hydrogen-storage technology. Since the dissociative adsorption of gaseous hydrogen molecules is the rate-limiting process among the whole hydrogen transport processes in hydrogen absorption into metals in many metal-hydrogen systems,[46,50,51] an active dissociation of hydrogen molecules by applied electric field may, for instance, significantly enhance the total hydrogen absorption velocity into solid metals. In this scheme, the applied electric field will be particularly enhanced in the vicinity of the metal surfaces, where the atomic dissociation occurs most efficiently for the subsequent surface adsorption due to the surface-plasmon effect. In addition, such a plasmonic field enhancement scheme on metal surfaces can also be utilized for the enhancement of the sensitivity of hydrogen detection.[14–16]

This plasmonic field enhancement effect also has the potential to be applied to nuclear-fusion technologies. A potential application for such scenario of nuclear-fusion phenomenon supported by the plasmonic field enhancement effect is illustrated as follows. Once an initial nuclear-fusion reaction occurs in the highly

concentrated energetic "hot spot" region around a metal surface, the heat locally generated by the nuclear reaction induces subsequent reactions around the region and thus effectively initiates heat-mediated chain reactions to spread throughout the fuel material. Such "hot spots" can trigger an initial nuclear-fusion reaction to locally generate large amounts of heat and induce subsequent reactions by supplying the necessary activation energy, thereby leading to a complete fusion ignition of the entire fuel material. The local energy-focusing effect studied in this paper thus significantly increases the probability of the initial nuclear reaction, even if the total power supplied to the fuel material remains the same, and, therefore, may effectively reduce the input power threshold.

For laser fusion, we previously proposed and analyzed an efficient ignition system comprising metal nanoparticles or nanoshells embedded in conventional deuterated polystyrene fuel targets.[39] Our present results further indicate an additional scheme for a novel type of fuel target for deuterium- or tritium-absorbed transition-metal-based materials. It should be noted that a combination of the field-enhancement scheme proposed in this paper with the existing metal-cone guiding scheme[18,19] may potentially enhance the overall energy-coupling efficiency even further.

In the lower frequency region, in particular, high-level field enhancement is attainable for Pd, Ti, and Ni, which are commonly used for condensed-matter fusion, as seen in Fig. 3. It is important to note that a certain number of the electrolysis-type condensed-matter nuclear-fusion experiments reported so far[22–25] may actually have benefited from this plasmonic local energy enhancement effect. If the spatial density of the reactive sites and the nuclear-reaction probability had been sufficiently high, the fuel samples would have been highly energy-absorptive. Therefore, the given incident energy would almost have been perfectly absorbed and converted for the reaction excitation. As a result, the electromagnetic enhancement effect presented in this work would hardly have contributed to the nuclear-reaction rate. In reality, however, the situation seen in many experimental reports in the community is likely the very opposite, and, therefore, the enhancement of the density of the supplied energy around the nuclear-reaction sites would increase the reaction rates by providing a larger opportunity for, and a larger amount of energy to be absorbed and consequently utilized for the excitation. For the external-field coupling into the surface-plasmon modes mentioned earlier, the possibility of the existence of intrinsic micro/nanoscale roughness or roughness induced in the electrolytic processes on metal surfaces in past experimental works is easily assumed. It is, therefore, supposed that there is some surface-plasmon electromagnetic enhancement effect even for metal plate samples, not to mention for the metal samples with micro/nanostructures with the abovementioned plasmon-coupling mechanism. It is highly possible that the plasmonic enhancement effect is partly responsible for the micro/nanostructures of samples used with many of the successful experimental reports.[25–27] Another evidence for this speculative plasmonic boosting effect is that there have been a number of successful experimental reports with the application of alternative or modulated electrical bias rather than stationary field particularly in D_2O,[24,52,53] which may have unknowingly excited the surface-plasmon oscillation, as Fig. 3(b) shows larger field enhancement at higher frequencies. The field-enhancement phenomenon studied, thus, could provide some clue toward solving the mystery of the energy supplied in overcoming the gigantic Coulomb barrier needed to produce the fusion reaction observed with visible rates, as well as a powerful tool for further technical progress.

IV. CONCLUSIONS

In this work, we quantitatively investigated the enhancement of electromagnetic energy density around planar metal surfaces. We found that a large degree of enhancement, which is even higher than those for noble metals, is available for hydrogen-absorbing transition metals (Pd, Ti, and Ni) in the microwave region. The calculation scheme and results presented in this paper could be a useful tool for the design, analysis, and optimization of the hydrogen-related systems and their operation conditions, to efficiently harvest the plasmonic boosting effect. The calculated plasmonic field enhancement effect can thus be utilized for the improvement of practical energy-storing and energy-generating devices, such as those for hydrogen storage, sensing, and nuclear fusion.

ACKNOWLEDGMENTS

This work was financially supported, in part, by the Thermal & Electric Energy Technology Foundation and the Research Foundation for Opto-Science and Technology.

APPENDIX: FUNCTIONAL FITS TO DIELECTRIC CONSTANT DATA

ε': real part of dielectric function
ε'': imaginary part of dielectric function
λ: freespace wavelength in micrometer

Au

$$\varepsilon' = 0.014\,861\,1\lambda^6 - 0.591\,797\,9\lambda^5 + 9.172\,669\lambda^4 - 67.718\,35\lambda^3 + 218.3918\lambda^2 - 473.2765\lambda + 329.5021$$
$(2.066\,\mu\text{m} < \lambda < 9.919\,\mu\text{m})$

$$\varepsilon'' = -0.003\,199\,534\lambda^6 + 0.103\,441\,5\lambda^5 - 1.431\,654\lambda^4 + 11.350\,59\lambda^3 - 34.742\,65\lambda^2 + 71.362\,84\lambda - 53.754\,34$$
$(2.066\,\mu\text{m} < \lambda < 9.919\,\mu\text{m})$

Ag

$$\varepsilon' = -0.004\,344\,238\lambda^6 + 0.126\,846\,3\lambda^5 - 1.473\,844\lambda^4 + 11.990\,35\lambda^3 - 97.026\,11\lambda^2 + 151.3469\lambda - 142.0007$$
$(2.066\,\mu\text{m} < \lambda < 9.919\,\mu\text{m})$

$$\varepsilon'' = 0.018\,851\,39\lambda^6 - 0.652\,647\,3\lambda^5 + 8.807\,471\lambda^4 - 58.246\,93\lambda^3 + 216.8512\lambda^2 - 394.5561\lambda + 284.2413$$
$(2.066\,\mu\text{m} < \lambda < 9.919\,\mu\text{m})$

Cu

$$\varepsilon' = -0.005\,803\,838\lambda^6 + 0.216\,297\,5\lambda^5 - 2.965\,184\lambda^4 + 20.810\,73\lambda^3 - 105.5591\lambda^2 + 139.8992\lambda - 94.139\,01$$
$(1.240\,\mu\text{m} < \lambda < 9.537\,\mu\text{m})$

$$\varepsilon'' = -0.007\,910\,679\lambda^6 + 0.230\,782\lambda^5 - 2.709\,187\lambda^4 + 16.918\,62\lambda^3 - 44.9983\lambda^2 + 66.4749\lambda - 33.765\,91$$
$(1.240\,\mu\text{m} < \lambda < 9.537\,\mu\text{m})$

Pd
$\varepsilon' = -66.630\,43\lambda^6 + 513.3435\lambda^5 - 1552.611\lambda^4 + 2349.634\lambda^3 - 1884.806\lambda^2 + 724.2406\lambda - 112.9396$
$(1.240\,\mu m < \lambda < 2.296\,\mu m)$
$\varepsilon' = -0.001\,713\,934\lambda^6 + 0.093\,379\,73\lambda^5 - 2.018\,558\lambda^4 + 22.266\,73\lambda^3 - 152.1131\lambda^2 + 408.1293\lambda - 462.8617$
$(2.296\,\mu m < \lambda < 12.40\,\mu m)$
$\varepsilon'' = 11.336\,71\lambda^6 - 108.7595\lambda^5 + 410.8409\lambda^4 - 775.3821\lambda^3 + 769.734\lambda^2 - 344.5274\lambda + 65.548\,76$
$(1.240\,\mu m < \lambda < 2.583\,\mu m)$
$\varepsilon'' = -0.010\,045\,35\lambda^6 + 0.435\,852\,9\lambda^5 - 7.514\,81\lambda^4 + 65.628\,38\lambda^3 - 302.1163\lambda^2 + 703.3077\lambda - 542.222$
$(2.583\,\mu m < \lambda < 12.40\,\mu m)$

Ti
$\varepsilon' = 5.269\,995\,36\lambda^6 - 49.049\,243\lambda^5 + 158.705\,051\lambda^4 - 183.980\,249\lambda^3 - 49.559\,521\,5\lambda^2 + 254.098\,657\lambda - 138.054\,204$
$(1.240\,\mu m < \lambda < 3.180\,\mu m)$
$\varepsilon' = -553.370\,717\lambda^6 + 12\,062.7911\lambda^5 - 109\,417.793\lambda^4 + 528\,601.697\lambda^3 - 1\,434\,430.74\lambda^2 + 2\,073\,005.55\lambda - 1\,246\,424.61$
$(3.180\,\mu m < \lambda < 4.130\,\mu m)$
$\varepsilon' = 125.124\,326\lambda^6 - 3929.427\,04\lambda^5 + 51\,337.6228\lambda^4 - 357\,165.883\lambda^3 + 1\,395\,575.74\lambda^2 - 2\,903\,797.3\lambda + 2\,513\,642.97$
$(4.130\,\mu m < \lambda < 6.000\,\mu m)$
$\varepsilon' = -0.000\,000\,007\,989\,052\,65\lambda^6 + 0.000\,004\,900\,123\,72\lambda^5 - 0.001\,146\,064\,52\lambda^4 + 0.125\,527\,4\lambda^3 - 5.905\,607\,11\lambda^2 + 6.477\,109\,46\lambda + 49.426\,199\,9$
$(6.000\,\mu m < \lambda < 200.0\,\mu m)$
$\varepsilon'' = 19.9751\lambda^6 - 309.7294\lambda^5 + 1948.945\lambda^4 - 6343.577\lambda^3 + 11\,216.39\lambda^2 - 10\,178.31\lambda + 3726.513$
$(1.240\,\mu m < \lambda < 4.130\,\mu m)$
$\varepsilon'' = 0.236\,713\,7\lambda^6 - 9.155\,287\lambda^5 + 145.3041\lambda^4 - 1210.59\lambda^3 + 5583.728\lambda^2 - 13\,507.74\lambda + 13\,399.26$
$(4.130\,\mu m < \lambda < 8.860\,\mu m)$
$\varepsilon'' = -0.000\,166\,523\,659\lambda^6 + 0.011\,065\,571\,1\lambda^5 - 0.236\,439\,095\lambda^4 + 0.767\,357\,479\lambda^3 + 39.034\,185\,2\lambda^2 - 484.302\,483\lambda + 1738.669\,36$
$(8.860\,\mu m < \lambda < 22.20\,\mu m)$
$\varepsilon'' = 0.000\,000\,002\,373\,964\lambda^6 - 0.000\,001\,762\,318\lambda^5 + 0.000\,531\,104\,4\lambda^4 - 0.082\,902\,81\lambda^3 + 6.994\,269\lambda^2 - 95.019\,41\lambda + 312.4735$
$(22.20\,\mu m < \lambda < 200.0\,\mu m)$

Ni
$\varepsilon' = -0.000\,730\,197\,274\,236\,8\lambda^6 + 0.021\,762\,436\,300\,37\lambda^5 - 0.157\,603\,136\,501\lambda^4 - 0.543\,551\,132\,632\,4\lambda^3 - 5.218\,665\,643\,26\lambda^2 - 13.774\,141\,605\,99\lambda + 2.145\,675\,254\,47$
$(1.240\,\mu m < \lambda < 12.40\,\mu m)$
$\varepsilon'' = 0.001\,869\,225\lambda^6 - 0.073\,607\,83\lambda^5 + 1.084\,908\lambda^4 - 6.738\,122\lambda^3 + 17.294\,31\lambda^2 + 15.815\,91\lambda - 0.226\,482$
$(1.240\,\mu m < \lambda < 12.40\,\mu m)$

H_2O
$\varepsilon' = 0.033\,794\,88\lambda^6 - 0.425\,524\,8\lambda^5 + 1.911\,36\lambda^4 - 4.066\,653\lambda^3 + 4.350\,977\lambda^2 - 2.252\,962\lambda + 2.215\,805$
$(1.24\,\mu m < \lambda < 2.80\,\mu m)$
$\varepsilon' = -0.166\,131\,5\lambda^6 + 4.571\,909\lambda^5 - 51.972\,92\lambda^4 + 312.201\lambda^3 - 1044.509\lambda^2 + 1844.044\lambda - 1339.195$
$(2.80\,\mu m < \lambda < 5.90\,\mu m)$
$\varepsilon' = -0.000\,170\,891\lambda^6 + 0.010\,646\,31\lambda^5 - 0.271\,335\,6\lambda^4 + 3.623\,13\lambda^3 - 26.751\,36\lambda^2 + 103.5364\lambda - 162.2594$
$(5.90\,\mu m < \lambda < 15.5\,\mu m)$
$\varepsilon' = -0.000\,000\,010\,265\,09\lambda^6 + 0.000\,002\,099\,101\lambda^5 - 0.000\,174\,955\,4\lambda^4 + 0.007\,696\,468\lambda^3 - 0.191\,96\lambda^2 + 2.627\,545\lambda - 13.393\,26$
$(15.5\,\mu m < \lambda < 50.0\,\mu m)$
$\varepsilon' = 0.000\,000\,000\,004\,202\,5\lambda^6 - 0.000\,000\,003\,076\,793\lambda^5 + 0.000\,000\,893\,753\,8\lambda^4 - 0.000\,129\,954\,1\lambda^3 + 0.009\,669\,09\lambda^2 - 0.312\,288\,4\lambda + 5.228\,968$
$(50.0\,\mu m < \lambda < 200\,\mu m)$
$\varepsilon'' = 0.039\,600\,00/(\lambda - 3.0) - 0.022\,000\,00$
$(1.24\,\mu m < \lambda < 2.95\,\mu m)$
$\varepsilon'' = 0.246\,115\,3/(\lambda - 2.7) - 0.214\,461\,2$
$(2.95\,\mu m < \lambda < 3.80\,\mu m)$
$\varepsilon'' = -0.035\,136\,00/(\lambda - 6.2) - 0.005\,360\,000$
$(3.80\,\mu m < \lambda < 6.10\,\mu m)$
$\varepsilon'' = 0.000\,149\,334\,8\lambda^6 - 0.009\,732\,903\lambda^5 + 0.259\,123\lambda^4 - 3.604\,89\lambda^3 + 27.651\,39\lambda^2 - 110.964\,3\lambda + 182.2369$
$(6.10\,\mu m < \lambda < 15.5\,\mu m)$
$\varepsilon'' = -0.000\,000\,016\,363\,05\lambda^6 + 0.000\,003\,351\,77\lambda^5 - 0.000\,282\,315\,6\lambda^4 + 0.012\,519\,61\lambda^3 - 0.306\,665\,4\lambda^2 + 3.895\,341\lambda - 18.7172$
$(15.5\,\mu m < \lambda < 50.0\,\mu m)$
$\varepsilon'' = -0.000\,000\,000\,006\,406\,405\lambda^6 + 0.000\,000\,005\,033\,237\lambda^5 - 0.000\,001\,602\,807\lambda^4 + 0.000\,264\,475\,3\lambda^3 - 0.023\,826\,71\lambda^2 + 1.110\,536\lambda - 18.837\,38$
$(50.0\,\mu m < \lambda < 200\,\mu m)$

REFERENCES

[1] L. Schlapbach and A. Zuttel, Nature **414**, 353 (2001).
[2] B. D. Adams and A. Chen, Mater. Today **14**, 282 (2011).
[3] G. Li, H. Kobayashi, J. M. Taylor, R. Ikeda, Y. Kubota, K. Kato, M. Takata, T. Yamamoto, S. Toh, S. Matsumura, and H. Kitagawa, Nat. Mater. **13**, 802 (2014).
[4] R. Mohtadi and S. Orimo, Nat. Rev. Mater. **2**, 16091 (2017).
[5] F. Favier, E. C. Walter, M. P. Zach, T. Benter, and R. M. Penner, Science **293**, 2227 (2001).
[6] R. H. Ritchie, Phys. Rev. **106**, 874 (1957).
[7] M. Ihara, K. Tanaka, K. Sakaki, I. Honma, and K. Yamada, J. Phys. Chem. B **101**, 5153 (1997).
[8] W. L. Barnes, A. Dereux, and T. W. Ebbesen, Nature **424**, 824 (2003).
[9] K. Okamoto, I. Niki, A. Shvartser, Y. Narukawa, T. Mukai, and A. Scherer, Nat. Mater. **3**, 601 (2004).
[10] K. Tanabe, J. Phys. Chem. C **112**, 15721 (2008).
[11] K. Nakayama, K. Tanabe, and H. A. Atwater, Appl. Phys. Lett. **93**, 121904 (2008).
[12] K. Tanabe, Nanoscale Res. Lett. **11**, 236 (2016).
[13] K. Tanabe, Grant application (unpublished).
[14] C. Langhammer, I. Zoric, B. Kasemo, and B. M. Clemens, Nano Lett. **7**, 3122 (2007).
[15] A. Baldi, T. C. Narayan, A. L. Koh, and J. A. Dionne, Nat. Mater. **13**, 1143 (2014).
[16] A. Ulvestad, M. J. Welland, W. Cha, Y. Liu, J. W. Kim, R. Harder, E. Maxey, J. N. Clark, M. J. Highland, H. You, P. Zapol, S. O. Hruszkewycz, and G. B. Stephenson, Nat. Mater. **16**, 565 (2017).
[17] J. Nuckolls, L. Wood, A. Thiessen, and G. Zimmerman, Nature **239**, 139 (1972).

[18]R. Kodama, P. A. Norreys, K. Mima, A. E. Dangor, R. G. Evans, H. Fujita, Y. Kitagawa, K. Krushelnick, T. Miyakoshi, N. Miyanaga, T. Norimatsu, S. J. Rose, T. Shozaki, K. Shigemori, A. Sunahara, M. Tampo, K. A. Tanaka, Y. Toyama, T. Yamanaka, and M. Zepf, Nature **412**, 798 (2001).
[19]R. Kodama and the Fast-Ignitor Consortium, Nature **418**, 933 (2002).
[20]Y. Mori, Y. Nishimura, R. Hanayama, S. Nakayama, K. Ishii, Y. Kitagawa, T. Sekine, N. Sato, T. Kurita, T. Kawashima, H. Kan, O. Komeda, T. Nishi, H. Azuma, T. Hioki, T. Motohiro, A. Sunahara, Y. Sentoku, and E. Miura, Phys. Rev. Lett. **117**, 055001 (2016).
[21]S. Le Pape, L. F. Berzak Hopkins, L. Divol, A. Pak, E. L. Dewald, S. Bhandarkar, L. R. Bennedetti, T. Bunn, J. Biener, J. Crippen, D. Casey, D. Edgell, D. N. Fittinghoff, M. Gatu-Johnson, C. Goyon, S. Haan, R. Hatarik, M. Havre, D. D. Ho, N. Izumi, J. Jaquez, S. F. Khan, G. A. Kyrala, T. Ma, A. J. Mackinnon, A. G. MacPhee, B. J. MacGowan, N. B. Meezan, J. Milovich, M. Millot, P. Michel, S. R. Nagel, A. Nikroo, P. Patel, J. Ralph, J. S. Ross, N. G. Rice, D. Strozzi, M. Stadermann, P. Volegov, C. Yeamans, C. Weber, C. Wild, D. Callahan, and O. A. Hurricane, Phys. Rev. Lett. **120**, 245003 (2018).
[22]M. Fleischmann, S. Pons, and M. Hawkins, J. Electroanal. Chem. **261**, 301 (1989).
[23]S. E. Jones, E. P. Palmer, J. B. Czirr, D. L. Decker, G. L. Jensen, J. M. Thorne, S. F. Taylor, and J. Rafelski, Nature **338**, 737 (1989).
[24]N. Wada and K. Nishizawa, Jpn. J. Appl. Phys. **28**, L2017 (1989).
[25]Y. Arata and Y. Zhang, Jpn. J. Appl. Phys. **38**, L774 (1999).
[26]Y. Iwamura, M. Sakano, and T. Itoh, Jpn. J. Appl. Phys. **41**, 4642 (2002).
[27]T. Hioki, N. Takahashi, S. Kosaka, T. Nishi, H. Azuma, S. Hibi, Y. Higuchi, A. Murase, and T. Motohiro, Jpn. J. Appl. Phys. **52**, 107301 (2013).
[28]A. L. Lereu, F. Lemarchand, M. Zerrad, M. Yazdanpanah, and A. Passian, J. Appl. Phys. **117**, 063110 (2015).
[29]J. B. Pendry, A. J. Holden, W. J. Stewart, and I. Youngs, Phys. Rev. Lett. **76**, 4773 (1996).
[30]D. R. Smith, D. C. Vier, W. Padilla, S. C. Nemat-Nasser, and S. Schultz, Appl. Phys. Lett. **75**, 1425 (1999).
[31]M. J. Lockyear, A. P. Hibbins, and J. Roy Sambles, Phys. Rev. Lett. **102**, 073901 (2009).
[32]K. Tanabe, J. Condens. Matter Nucl. Sci. **27**, 152 (2018).
[33]W. H. Weber and G. W. Ford, Opt. Lett. **6**, 122 (1981).
[34]S. L. Westcott, J. B. Jackson, C. Radloff, and N. J. Halas, Phys. Rev. B **66**, 155431 (2002).
[35]N. K. Grady, N. J. Halas, and P. Nordlander, Chem. Phys. Lett. **399**, 167 (2004).
[36]G. M. Hale and M. R. Querry, Appl. Opt. **12**, 555 (1973).
[37]*Handbook of Optical Constants of Solids*, edited by E. D. Palik (Academic Press, Orlando, FL, 1985).
[38]C. F. Bohren and D. R. Huffman, *Absorption and Scattering of Light by Small Particles* (Wiley-VCH, Weinheim, 1983), Chaps. 3 and 5.
[39]K. Tanabe, Jpn. J. Appl. Phys. **55**, 08RG01 (2016).
[40]H. Raether, *Surface Plasmons on Smooth and Rough Surfaces and on Gratings* (Springer, Berlin, 1988).
[41]J. B. Pendry, L. Martin-Moreno, and F. J. Garcia-Vidal, Science **305**, 847 (2004).
[42]D. Pacifici, H. J. Lezec, L. A. Sweatlock, R. J. Walters, and H. A. Atwater, Opt. Express **16**, 9222 (2008).
[43]F. Toigo, A. Marvin, V. Celli, and N. R. Hill, Phys. Rev. B **15**, 5618 (1977).
[44]K. Arya, Z. B. Su, and J. L. Birman, Phys. Rev. Lett. **54**, 1559 (1985).
[45]K. Tanabe, Heliyon **2**, e00057 (2016).
[46]Y. Kitagawa and K. Tanabe, Chem. Phys. Lett. **699**, 132 (2018).
[47]K. H. Su, Q. H. Wei, X. Zhang, J. J. Mock, D. R. Smith, and S. Schultz, Nano Lett. **3**, 1087 (2003).
[48]D. F. P. Pile, T. Ogawa, D. K. Gramotnev, Y. Matsuzaki, K. C. Vernon, K. Yamaguchi, T. Okamoto, M. Haraguchi, and M. Fukui, Appl. Phys. Lett. **87**, 261114 (2005).
[49]J. A. Dionne, L. A. Sweatlock, H. A. Atwater, and A. Polman, Phys. Rev. B **73**, 035407 (2006).
[50]T. Mitsui, M. K. Rose, E. Fomin, D. F. Ogletree, and M. Salmeron, Nature **422**, 705 (2003).
[51]N. Lopez, Z. Lodziana, F. Illas, and M. Salmeron, Phys. Rev. Lett. **93**, 146103 (2004).
[52]J. R. Granada, R. E. Mayer, G. Guido, P. C. Florido, A. Larreteguy, V. H. Gillette, N. E. Patino, J. Converti, and S. E. Gomez, J. Nucl. Sci. Technol. **27**, 222 (1990).
[53]A. Takahashi, T. Takeuchi, T. Iida, and M. Watanabe, J. Nucl. Sci. Technol. **27**, 663 (1990).